# Multiferroic properties of $Ni_{0.5}Zn_{0.5}Fe_2O_4$–$Pb(Zr_{0.53}Ti_{0.47})O_3$ ceramic composites

Hongfang Zhang,[1] Siu Wing Or,[1,2,a)] and Helen Lai Wa Chan[1]
[1]*Department of Applied Physics, The Hong Kong Polytechnic University, Hung Hom, Kowloon, Hong Kong*
[2]*Department of Electrical Engineering, The Hong Kong Polytechnic University, Hung Hom, Kowloon, Hong Kong*

(Received 11 May 2008; accepted 5 October 2008; published online 19 November 2008)

We present a powder-in-sol precursor hybrid processing route to synthesize dense, homogenous, and fine-grained $Ni_{0.5}Zn_{0.5}Fe_2O_4$–$Pb(Zr_{0.53}Ti_{0.47})O_3$ (NZFO–PZT) multiferroic ceramic composites and report their ferromagnetic-ferroelectric characteristics. Nanosized NZFO ferromagnetic powders are dispersed into PZT ferroelectric sol-gel precursor and uniformly distributed slurry is prepared by ball-milling mixing of the powder-precursor suspension prior to be sintered at low temperatures to form the composites. The composites show simultaneous effects of ferromagnetism and ferroelectricity at room temperature with excellent magnetic and dielectric properties for frequencies over 10 MHz. The coexistence of inductive and capacitive natures in the composites favors size reduction and design simplification in many passive electronic devices such as integrated filters and microwave absorbers. © *2008 American Institute of Physics*. [DOI: 10.1063/1.3021349]

## I. INTRODUCTION

When ferromagnetism and ferroelectricity coexist in a single material, multiferroicity due to the interactions between magnetization and electric polarization occurs.[1–3] While the multiferroic effect is both physically interesting and technologically important, only a few single-phase materials are found to exhibit both spontaneous magnetization and electric polarization at room temperature.[4,5] Accordingly, various processes have been developed in the recent years to synthesize ferromagnetic-ferroelectric-based multiferroic ceramic composites.[6–8] Among them, solid-state mixed powder sintering is a more beneficial process because it is not only relatively simple and cost effective but also allows the adjustments of the molar ratio and grain size of each phase and the sintering temperature of the composites.[9] Nevertheless, there are three technical issues that should be addressed prior to the success synthesis of high-quality composites based on the approach. First, chemical reactions between the ferromagnetic and ferroelectric phases in the composites during sintering should be avoided as they are inclined to deteriorate the properties of the composites. Second, the electric resistivity of the ferromagnetic phase should be as high as possible so as to minimize leakage currents and prevent the composites from electric breakdown during poling of their ferroelectric phase. In fact, when the ferromagnetic phase in the composites connects in a chainlike manner, the electric resistivity of the composites will be greatly reduced. Hence, it is highly desirable to uniformly disperse the ferromagnetic phase in the composites. Third, mechanical defects, such as pores at the interfaces of the ferromagnetic and ferroelectric phases, should be avoided to ensure good mechanical coupling to the phases.

In this paper, a powder-in-sol precursor hybrid processing route, which essentially combines the advantages of conventional solid-state ceramic process and those of sol-gel wet chemistry process, is introduced to alleviate the problems/deficiencies intrinsic in synthesizing ferromagnetic-ferroelectric-based multiferroic ceramic composites. The route includes (1) the dispersion of nanosized $Ni_{0.5}Zn_{0.5}Fe_2O_4$ (NZFO) ferromagnetic powders (acting as the filler) prepared by conventional solid-state ceramics process into $Pb(Zr_{0.53}Ti_{0.47})O_3$ (PZT) ferroelectric sol-gel precursor (acting as the matrix) prepared via sol-gel wet chemistry process, (2) the mixing of the powder-precursor suspension by ball milling to form uniformly distributed slurry, and (3) the sintering of the slurry at low temperatures to produce dense, homogenous, and fine-grained composites with attractive multiferroic characteristics. This hybrid process has been developed by grafting the conventional solid-state ceramic process onto the sol-gel wet chemistry process, thereby combining the advantageous features of high crystallinity and high performance associated with the conventional solid-state ceramic process with those of the fine grain character and low sintering temperature heritage from the sol-gel wet chemistry process. This processing route is effective in synthesizing ferromagnetic-ferroelectric-based multiferroic ceramic composites. In the following sections, we describe the processing route, sintering behavior, microstructures, ferromagnetic behavior, and magnetic properties, as well as ferroelectric behavior and dielectric properties of the NZFO–PZT multiferroic ceramic composites.

## II. EXPERIMENTS

### A. Processing route for preparing uniformly distributed slurry

The nanosized NZFO ferromagnetic powders were prepared by conventional solid-state ceramic process. Commercial iron oxide ($Fe_2O_3$), zinc oxide (ZnO), and nickel oxide (NiO), each with 99.5% purity, were mixed thoroughly and

a)Author to whom correspondence should be addressed. Electronic mail: eeswor@polyu.edu.hk.

 © 2008 American Institute of Physics

Downloaded 16 Mar 2011 to 158.132.161.180. Redistribution subject to AIP license or copyright; see http://jap.aip.org/about/rights_and_permissions

the mixture was calcined at 1000 °C for 4 h. The calcined NZFO powders were ball milled into nanosized powders with a size distribution of 20–100 nm using a high-energy planetary ball-milling machine (Frisch Pulverisette 5) with tungsten carbide milling jar and milling medium.

The PZT ferroelectric sol-gel precursor was prepared via sol-gel wet chemistry process. Commercial $Pb(CH_3COO)_2 \cdot 3H_2O$, $Zr[CH_3C(O)CHC(O)CH_3]_4$, and $Ti(OC_4H_9)_4$ were dissolved in 2-methoxyethanol according to the stoichiometric amount of PZT (with the mol ratio of 1:0.53:0.47). The solution was heated up to 80–90 °C with vigorous stirring for 2 h. The concentration of the PZT sol precursor was determined to be 0.4 M.

The as-prepared nanosized NZFO powders were dispersed into the PZT sol-gel precursor using three different mass ratios of NZFO powders to PZT sol-gel precursor of 25/75, 50/50, and 72/28 in order to balance the processing behavior and resulting properties of the composites. Each of the three powder-precursor suspensions was mixed by ball milling for 2 h to form uniformly distributed slurry looking like paint. These uniformly distributed slurries were ready for the synthesis of the NZFO–PZT ceramic composites to be described in the next section.

### B. Synthesis of multiferroic ceramic composites

Three different composites, namely, 25, 50, and 72 wt % composites based on the as-prepared uniformly distributed slurries with three different mass ratios of NZFO powders to PZT sol-gel precursor of 25/75, 50/50, and 72/28 were synthesized. Each of the three slurries was dried and calcined at 700 °C for 2 h to obtain granulated NZFO–PZT ceramic composite powders. The granulated powders were uniaxially pressed into either toroidal specimen with an outer diameter of 15 mm, an inner diameter of 6 mm, and a thickness of 3 mm at a pressure of 10 MPa or disk specimen with a diameter of 12 mm and a thickness of 1 mm at a pressure of 8 MPa, both in stainless steel dies. The pressed specimens were sintered in air at 1000–1100 °C for 4 h.

### C. Property measurements

The x-ray diffraction (XRD) patterns and microstructures of the composites at room temperature were characterized using an x-ray diffractometer (Philips X'Pert-Pro MPD) with Cu $K\alpha_1$ radiation (1.5406 Å, 40 kV, and 30 mA) and a field-emission scanning electron microscope (SEM) (JEOL JSM-6335F), respectively.

The magnetization-magnetic field hysteresis loops were measured using a vibrating sample magnetometer (Lakeshore 7300 series) at room temperature. The relative permeability and quality factor as a function of frequency were obtained by an impedance analyzer (Agilent 4294A) using coiled toroidal specimens.

The polarization-electric field hysteresis loops were evaluated using a modified Sawyer–Tower circuit at a frequency of 100 Hz at room temperature. The temperature dependences of relative permittivity at various frequencies were investigated at a heating rate of 2 °C/min using a computer-controlled automated system formed by the impedance analyzer, a temperature-controlled furnace (Carbolic), and a multimeter (Keithley 2000) as the temperature controller. The relative permittivity and loss tangent as a function of frequency were acquired by the impedance analyzer.

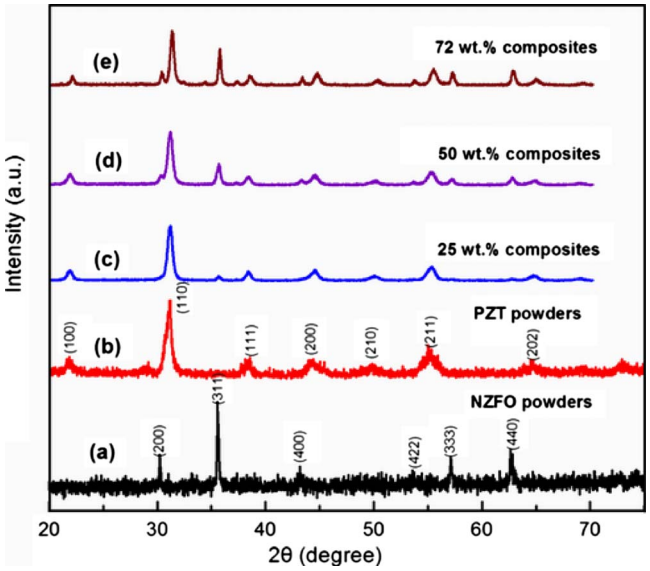


FIG. 1. (Color online) XRD patterns of (a) pure NZFO powders calcined at 1000 °C, (b) pure PZT powders calcined at 700 °C, (c) 25 wt % composites sintered at 1000 °C, (d) 50 wt % composites sintered at 1000 °C, and (e) 72 wt % composites sintered at 1000 °C.

## III. RESULTS AND DISCUSSION

### A. Sintering behavior and microstructures

Figure 1 shows the XRD patterns of the 25, 50, and 72 wt % composites sintered at 1000 °C for 4 h, together with the pure NZFO and PZT powders calcined at 1000 and 700 °C, respectively. The clear XRD patterns of NZFO and PZT powders indicate the presence of high purity and high crystallinity with a spinal structure in the pure NZFO powders [Fig. 1(a)] and a perovskite structure in the pure PZT powders [Fig. 1(b)]. The 25, 50, and 72 wt % composites in Figs. 1(c)–1(e) have their XRD peaks corresponding to their parental NZFO (the ferromagnetic phase) and PZT (the ferroelectric phase) powders.

Figure 2 illustrates the XRD patterns of the 50 wt % composites sintered at different temperatures of 900, 1000,

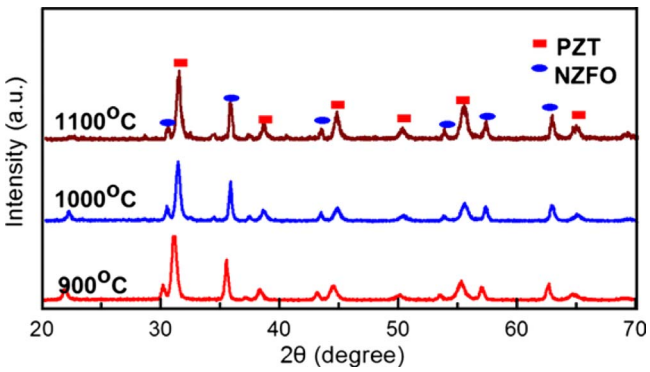


FIG. 2. (Color online) XRD patterns of 50 wt % composites sintered at different temperatures of 900, 1000, and 1100 °C.

Downloaded 16 Mar 2011 to 158.132.161.180. Redistribution subject to AIP license or copyright; see http://jap.aip.org/about/rights_and_permissions

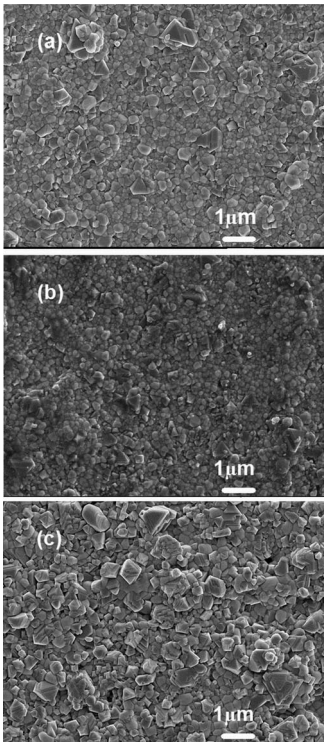


FIG. 3. Field-emission SEM micrographs of (a) 25 wt % composites sintered at 1000 °C, (b) 50 wt % composites sintered at 1000 °C, and (c) 72 wt % composites sintered at 1100 °C.

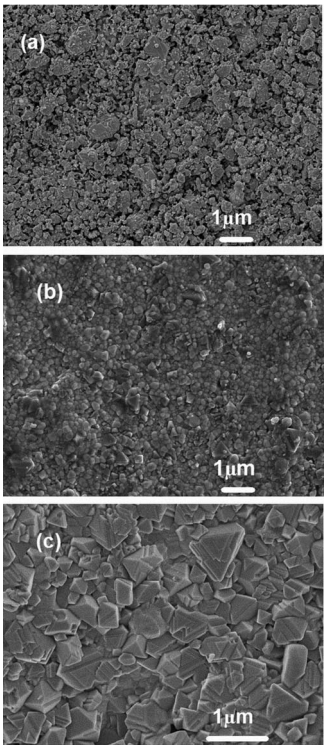


FIG. 4. Surface morphologies of 50 wt % composites sintered at (a) 900, (b) 1000, and (c) 1100 °C.

and 1100 °C in order to investigate if intermediate or interfacial phases are present in the composites or not. It is clear that the ferromagnetic NZFO phase with a typical spinal structure and the ferroelectric PZT phase with a typical tetragonal perovskite structure coexist in the composites for all sintering temperatures under study. The XRD peaks are identified with no detection of intermediate or interfacial phases. The results reflect the success in synthesizing composites with simultaneous ferroelectric and ferromagnetic phases using the proposed hybrid processing route.

Figure 3 displays the field-emission SEM micrographs of the 25 and 50 wt % composites sintered at 1000 °C and the 72 wt % composites sintered at 1100 °C. It is seen that the nanosized NZFO powders are uniformly distributed in the PZT sol-gel precursor with no observable mechanical defects, giving rise to dense, homogeneous, and fine-grained composites. The success in synthesizing such composites is mainly attributed to the strong adhesion between the NZFO powders and the PZT sol-gel precursor. In fact, surface hydroxyl groups are also present on the surface of the NZFO powders. The polymer species formed during hydrolysis and condensation of the sol-gel precursor are able to react with these surface hydroxyl groups and form strong bonds. Besides, the low crystallization temperature and less contraction during pyrolysis, crystallization, and sintering are essential in the production of high-quality ceramic composites. On the other hand, it is indeed practically difficult to obtain dense, homogeneous, and fine-grained ceramic composites by conventional solid-state ceramic process owing to the large differences in thermal expansion coefficient and sintering behaviors of NZFO and PZT components. As a result, nonuniform microstructures with large and different grain sizes and severe pores result instead. Nevertheless, such undesirable phenomena are not evident in our composites synthesized via the novel hybrid processing route. It is known that fine grain size can effectively reduce the residual stresses and inhibit the occurrence of mechanical defects in the composites during sintering.[10] In this hybrid processing route, the sol-gel matrix essentially acts as a buffer to inhibit the grain growth. Hence, the final grains are in submicron size and the sintering temperatures are relatively low. These are the most attractive features of the route.

Figure 4 shows the surface morphologies of the 50 wt % composites sintered at various temperatures of 900, 1000, and 1100 °C. With increasing the sintering temperature from 900 to 1100 °C, densification of the composites takes place. The grain sizes and grain distributions of NZFO and PZT are almost the same with no apparent grain growth for the sintering temperatures up to 1000 °C [Figs. 4(a) and 4(b)]. The average grain sizes of the NZFO and PZT phases are found to be about 200 nm. Dense, homogeneous, and fine-grained composites with no intermediate or interfacial phases are obtained at 1000 °C [Fig. 4(b)], as confirmed by the corresponding XRD pattern in Fig. 2. At an increased sintering temperature of 1100 °C [Fig. 4(c)], the grain growth becomes bigger with an increased average grain size less than 1 $\mu$m. Considering the original size of the NZFO powders of 20–100 nm, the relatively larger size grain implies that the phase development in the composites is as follows. First, during the early stage of the sintering, nucleation initiates from the sol-gel amorphous phase (PZT). The nuclei grow up until all the resultant crystallites begin to impinge on one another. Thus, the sol-gel derived crystallites are con-

Downloaded 16 Mar 2011 to 158.132.161.180. Redistribution subject to AIP license or copyright; see http://jap.aip.org/about/rights_and_permissions

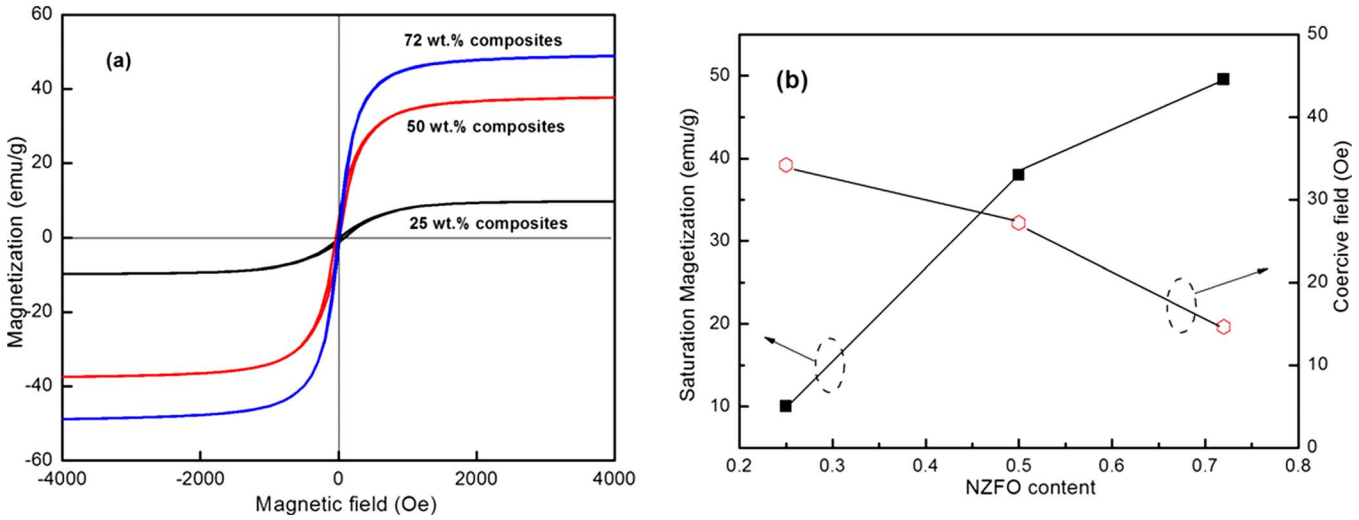


FIG. 5. (Color online) (a) Magnetization-magnetic field hysteresis loops of the 25 and 50 wt % composites sintered at 1000 °C and the 72 wt % composites sintered at 1100 °C and (b) their saturation magnetizations and coercive fields.

nected to the powders (NZFO) to form aggregates and leave some voids within the interstices between the aggregates. With further heating, the aggregates are easily developed into large size grains. That is why we get the uniformly distributed grains with sizes around 200 nm in the above-mentioned morphologies at 1000 °C. With further increasing sintering temperature, the newly formed grains further grow up as a common sense.

### B. Magnetic properties

Figure 5 shows the magnetization-magnetic field hysteresis loops of the 25 and 50 wt % composites sintered at 1000 °C and the 72 wt % composites sintered at 1100 °C, together with their saturation magnetizations and coercive fields. In Fig. 5(a), all composites exhibit typical ferromagnetic hysteresis loops, indicating the presence of ordered magnetic structure in the composites. For instance, the 50 wt % composites have saturation and remanent magnetizations of 37.993 and 1.707 emu/g, respectively. In Fig. 5(b), the saturation magnetization increases while the coercive field decreases with increasing NZFO content. The increase in saturation magnetization with increasing NZFO content provides an indication that the spontaneous magnetization of the composites, which originates from unbalanced antiparallel spins, leads to net spins other than those introduced by the structural distortion.[2] The decrease in coercive field with increasing NZFO content means that magnetization can be realized more easily with increasing NZFO content so that the interaction of the magnetic poles on the magnetic powders becomes energetic. The observation differs from a previous report.[11]

Figure 6 illustrates the relative permeability and quality factor as a function of frequency for the 25 wt % (that is 31% volume fraction of ferrite content) and 50 wt % (that is 57% volume fraction of ferrite content) composites sintered at 1000 °C and the 72 wt % (that is 78% volume fraction of ferrite content) composites sintered at 1100 °C. The relative permeability demonstrates excellent frequency stability throughout the whole measured frequency range, except for the variations associated with the parametric resonance of the

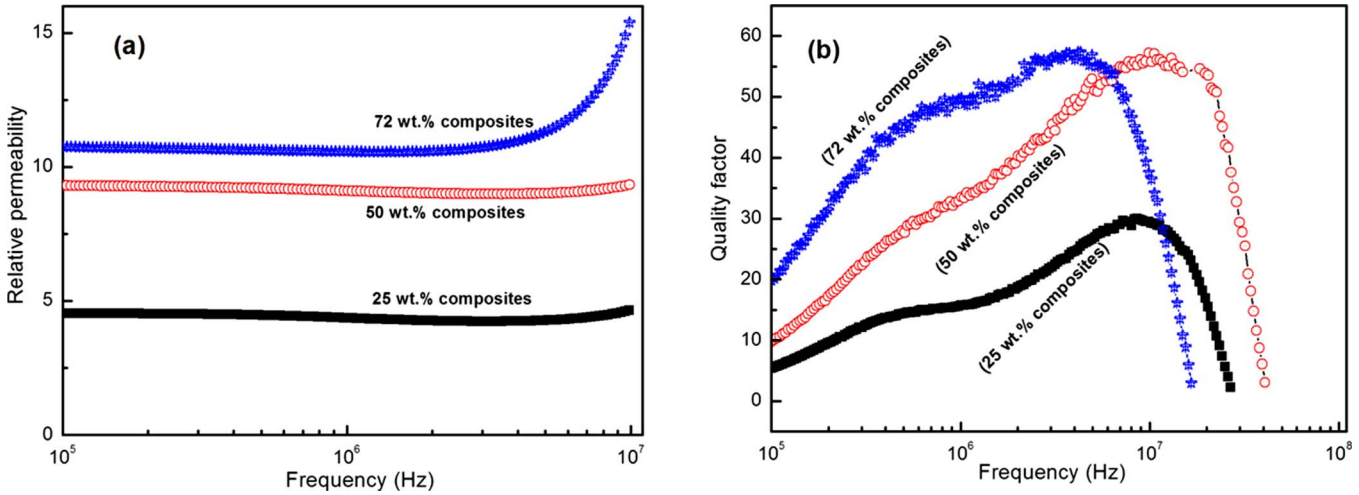


FIG. 6. (Color online) (a) Relative permeability and (b) quality factor as a function of frequency for the 25 and 50 wt % composites sintered at 1000 °C and the 72 wt % composites sintered at 1100 °C.

Downloaded 16 Mar 2011 to 158.132.161.180. Redistribution subject to AIP license or copyright; see http://jap.aip.org/about/rights_and_permissions

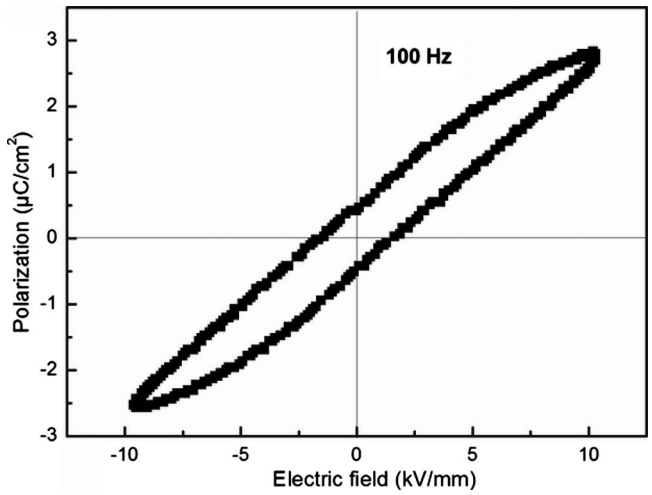


FIG. 7. Polarization-electric field hysteresis loop of the 50 wt % composites sintered at 1000 °C.

measurement circuit that appeared in the 72 wt % composites at frequencies above 10 MHz. By increasing NZFO content, the relative permeability and quality factor both increase with the peak associated with the quality factor shifting to lower frequencies. This tendency is consistent with Snoek's law[12] in that an increase in saturation magnetization leads to a decrease in the resonance frequency, and vice versa. Therefore, the relative permeability and cutoff frequency of the composites can be manipulated by changing the NZFO (or PZT) content.

### C. Electrical properties

Figure 7 plots the polarization-electric field hysteresis loop of the 50 wt % composites sintered at 1000 °C. The loop indicates ferroelectric behavior in the composites with remanent polarization and coercive field of 0.48 $\mu C/cm^2$ and 1.45 kV/mm, respectively. Although, at a first glance, the overall shape of the loop signifies that the loop is derived from a linear capacitor with high conduction; however, under careful examination, the saturation of the upper branch around the tip of the loop at high field is quite evident. Considering that the composites have NZFO/PZT volume ratio of 57/43, the high volume ratio of the NZFO phase with low dielectric constant and high conductivity dilute the ferroelectric characteristics of the PZT phase and dominate the overall characteristics of the hysteresis loop. Besides, the grain size of the PZT phase in the composite is very fine, resulting in a linearlike loop. We believe that the ferroelectric nature of the composites can be testified from this loop. As the composites show obvious ferromagnetism with good magnetic properties in Figs. 5 and 6, the coexistence of ferromagnetism and ferroelectricity in the composites at room temperature is thus confirmed here.

Figure 8(a) shows the temperature dependence of relative permittivity at 10 kHz for the 25 and 50 wt % composites sintered at 1000 °C and the 72 wt % composites sintered at 1100 °C, while Fig. 8(b) illustrates the temperature dependence of the relative permittivity for the 50 wt % composites at different frequencies of 1 kHz–1 MHz. For the 25 wt % composites in Fig. 8(a), the relative permittivity peaks at 390 °C, which is close to the Curie temperature of PZT of 660 K (387 °C). The peak becomes broader and shifts to lower temperatures for the 50 and 72 wt % composites with increased NZFO content. Moreover, the relative permittivity decreases with increasing NZFO content in the measured temperature range. The observations differ greatly from the literature[13] and suggest the contribution of the dielectric properties of the composites by the PZT phase. The fact that the temperature dependence of relative permittivity is so similar to that of the PZT provides a further proof of the presence of ferroelectricity in the composites. In Fig. 8(b), the composites exhibit a relaxer characteristic in that there is a shift in the peak of relative permittivity to the higher temperature side with increasing frequency. In relaxer materials, a sharp Curie transition transforms into diffused phase transition (DPT) and the relative permittivity is frequency dependent. PZT does not exhibit a relaxer characteristic but our composites show apparent relaxer characteristic. As a general understanding, the DPT is caused by cation disorder in com-

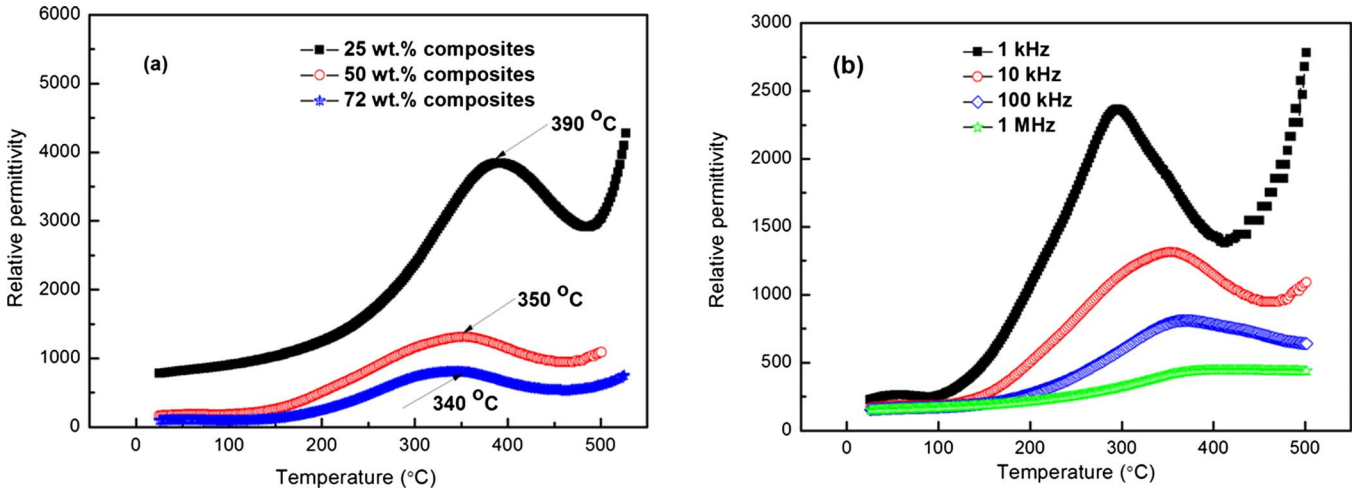


FIG. 8. (Color online) (a) Temperature dependence of relative permittivity at 10 kHz for 25 and 50 wt % composites sintered at 1000 °C and 72 wt % composites sintered at 1100 °C and (b) temperature dependence of the relative permittivity for the 50 wt % composites at different frequencies of 1 kHz–1 MHz.

Downloaded 16 Mar 2011 to 158.132.161.180. Redistribution subject to AIP license or copyright; see http://jap.aip.org/about/rights_and_permissions

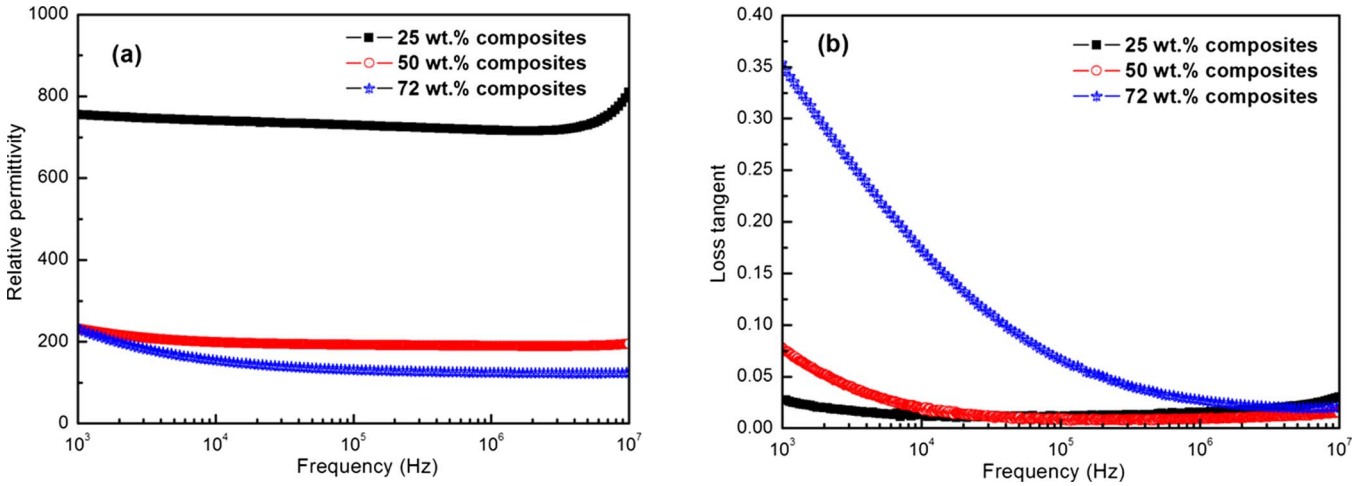


FIG. 9. (Color online) (a) Relative permittivity and (b) loss tangent as a function of frequency for the 25 and 50 wt % composites sintered at 1000 °C and the 72 wt % composites sintered at 1100 °C.

plex perovskite and is related to the nanoscaled ordered microregions in the material. The spontaneous polarization of the ordered microregions still survives above the average transition temperature.[14]

Figure 9 shows the relative permittivity and loss tangent as a function of frequency for the 25 and 50 wt % composites sintered at 1000 °C and the 72 wt % composites sintered at 1100 °C. The relative permittivity decreases while the loss tangent increases with increasing NZFO content. For example, the 25 wt % composites have a relative permittivity of 740 with a loss tangent of 0.01 at 10 kHz. By comparison, the 50 wt % composites have a reduced relative permittivity of 199 and an increased loss tangent of 0.02 at the same frequency. These values of loss tangent are about an order of magnitude lower than many reports using conventional solid-state ceramic process. It is noted from Fig. 9(a) that the relative permittivity of all composites is less frequency dependent in the range from 1 kHz to 10 MHz.[10]

## IV. CONCLUSION

Dense, homogenous, and fine-grained multiferroic ceramic composites consisting of nanosized NZFO ferromagnetic powders dispersed uniformly in PZT ferroelectric sol-gel precursor have been synthesized by a powder-in-sol precursor hybrid processing route. The coexistence of ferromagnetism and ferroelectricity has been confirmed by means of structural and morphological analyses as well as magnetization-magnetic field and polarization-electric field measurements. Excellent magnetic and dielectric properties have been observed for frequencies in excess of 10 MHz. The combined inductive and capacitive natures in the composites make the composites a promising candidate for design simplification and size minimization of many passive electronic devices such as integrated filters and microwave absorbers.

## ACKNOWLEDGMENTS

This work was supported by the Research Grants Council of the HKSAR Government under Grant No. PolyU 5122/05E and the Niche Areas Project of The Hong Kong Polytechnic University under Grant No. I-BB95.

[1]S. V. Suryanarayana, Bull. Mater. Sci. **17**, 1259 (1994); J. V. Such-telen, Philips Res. Rep. **27**, 28 (1972).
[2]T. Kanai, S. I. Ohkoshi A. Nakajima, T. Watanabe, and K. Hashimoto, Adv. Mater. (Weinheim, Ger.) **13**, 487 (2001).
[3]X. Qi, J. Zhou, B. Li, Y. Zhang, Z. Yue, Z. Gui, and L. T. Li, J. Am. Ceram. Soc. **87**, 1848 (2004).
[4]N. A. Hill, J. Phys. Chem. B **104**, 6694 (2000).
[5]M. Mahesh Kumar, V. R. Palkar, K. Srinivas, and S. V. Suryanarayana, Appl. Phys. Lett. **76**, 2764 (2000).
[6]G. L. Yuan, K. Z. Baba-Kishi, J.-M. Liu, S. W. Or, Y. P. Wang, and Z. G. Liu, J. Am. Ceram. Soc. **89**, 3136 (2006).
[7]Y. J. Wang, S. W. Or, H. L. W. Chan, X. Y. Zhao, and H. S. Luo, J. Appl. Phys. **103**, 124511 (2008).
[8]H. F. Zhang, S. W. Or, and H. L. W. Chan, Mater. Res. Innovations **12**, 142 (2008).
[9]W. Eerenstein, N. D. Mathur, and J. F. Scott, Nature (London) **442**, 759 (2006).
[10]W. G. Zhu, Z. H. Wang, C. L. Zhao, O. K. Tan, and H. H. Hng, Jpn. J. Appl. Phys., Part 1 **41**, 6969 (2002).
[11]X. Qi, J. Zhou, Z. X. Yue, Z. L. Gui, L. T. Li, and S. Buddhudu, Adv. Funct. Mater. **14**, 920 (2004).
[12]J. L. Snoek, Physica (Amsterdam) **14**, 207 (1948).
[13]J. Q. Huang, P. Y. Du, L. X. Hong, Y. L. Dong, and M. C. Hong, Adv. Mater. (Weinheim, Ger.) **19**, 437 (2007).
[14]L. E. Cross, Ferroelectrics **76**, 241 (1987).

Downloaded 16 Mar 2011 to 158.132.161.180. Redistribution subject to AIP license or copyright; see http://jap.aip.org/about/rights_and_permissions